Biogeosciences Discuss., https://doi.org/10.5194/bg-2018-385
Manuscript under review for journal Biogeosciences
Discussion started: 7 September 2018

Turbulence measurements suggest high rates of new production over the shelf edge in the north-eastern North Sea during summer

Jørgen Bendtsen[1], Katherine Richardson[2]

[1]ClimateLab, Symbion Science Park, Copenhagen, 2100 O, Denmark
[2]Center for Macroecology, Evolution and Climate, Natural History Museum of Denmark, University of Copenhagen, Copenhagen, 2100 O, Denmark

Correspondence to: Jørgen Bendtsen (jb@climatelab.dk)

Abstract. New production, i.e., that driven by allochthonous nutrient inputs, is the only form of primary production that can lead to net increases in organic material and is, therefore, important for understanding energy flow in marine ecosystems. The spatial distribution of new production is generally, however, not well known. Here, using data collected in July, 2016, we analyse the potential for vertical mixing to support new production in the upper layers of the north eastern portion of the North Sea. Estimated nitrate fluxes due to turbulent vertical mixing into the euphotic zone were up to 0.5 - 1 mmol N m^{-2} d^{-1} over the shelf-edge (f-ratios > 0.1) while values of < 0.1 mmol N m^{-2} d^{-1} were found in the deeper open area north of the shelf-edge. The low vertical mixing rates (dissipation rates of turbulent kinetic energy below 10^{-8} W kg^{-1}, corresponding to vertical turbulent diffusion coefficients of 10^{-6} - 10^{-5} m^2 s^{-1}) implied f-ratios of < 0.02 in the open waters north of the shelf-edge. In the shallow (< 50 m) southern and central part of the study area, inorganic nutrients were low and nitrate undetectable suggesting negligible new production here, despite relatively high concentrations of chlorophyll a being found in the bottom layer. Thus, high rates of new production seem generally during summer to be concentrated around the shelf-edge zone and in association with localized features exhibiting enhanced vertical mixing. Overall, this suggests that the shelf-edge zone was the major nutrient supplier to the euphotic zone in this area during summer.

1 Introduction

New Production (NP), i.e. primary production (PP) based on inorganic nutrients recently introduced to a system, balances net losses of organic material in the euphotic layer when considered over longer periods (Dugdale and Goering, 1967). Net loss of biomass from the surface layer may be due to sinking phytoplankton or transfer to, and subsequent losses from, higher trophic levels such that this cycle between nutrient input, PP and remineralisation of organic matter constitutes an organic biological pump in the upper ocean (Volk and Hoffert, 1987). In addition to NP, total PP is comprised of photosynthesis driven by nutrients recycled within the system, itself. The ratio of NP to total PP is referred to as the f-ratio (Eppley and Peterson, 1979). This ratio is known to vary both seasonally and spatially.

Like NP, the distribution of organisms representing higher trophic levels is also heterogeneous in the ocean and it has been suggested that the patchy distribution of apex predators may be related to the distribution of NP. Scott et al. (2010) analysed the distribution of marine mammals and seabirds in the north western North Sea. Those workers found the distribution of these organisms to be best explained by the presence of a sub-surface chlorophyll maximum (SCM) and speculated that bathymetric features induced vertical mixing bringing nutrients to depths containing the chlorophyll peak and leading, ultimately, to NP. This potential link between localized increased NP in sub-surface layers and the highest trophic levels may, therefore, be an important feature in ecosystem functioning. However, the distribution of NP, especially over small spatial scales, is not well understood. The purpose of this study, therefore, was to describe the potential for NP based on vertical mixing of nutrients from deeper waters into the euphotic zone to occur in the north eastern North Sea, a highly productive temperate ocean region. The summer season was chosen for the study as this region is thermally stratified at this time and surface waters characterized by low or undetectable concentrations of inorganic nutrients and low phytoplankton biomass. Thus, it is generally assumed that little NP is occurring in these waters at this time.

The north eastern North Sea is characterized by the transition from a relatively shallow southern region (depth ~ 40 m) across a shelf-edge (depth ~60 - 100 m) towards the deep (> 400 m) Norwegian Trench leading into Skagerrak (Fig. 1). The general cyclonic circulation is characterized by inflow from the Atlantic along the shelf-edge, either from mainly wind-driven inflow between the Shetland and Orkney Islands or from transports along the Norwegian Trench (Winther and Johannessen, 2006). Outflow takes place along the Norwegian coast, partly as less saline water masses in the Norwegian Coastal Current, and with an estimated net transport of about 1 Sv in either direction (Danielssen et al., 1990). The relatively large cyclonic flow has also been found in model studies (Winther and Johannessen, 2006; Pätch et al., 2017) where current speeds along the north eastern shelf-edge towards the Skagerrak intensifies (Holt and Proctor, 2008) and are found to be associated with a large eddy-activity (Røed and Fossum, 2004). This dynamic area is a potential location for increased vertical mixing and nutrient transports due to, for example, eddy-activity, breaking internal waves and upwelling at the shelf-edge and was, therefore, selected as the study area.

A large part of the central and northern North Sea becomes stratified during the summer season with an SCM between ~20-40 m depth. Richardson et al. (2000) found that a significant amount of PP occurs at the SCM and argued that much of this could be NP supported by fortnightly tidally driven input of nutrient rich deep water to the SCM. Fernand et al. (2013) found that up to 60% of PP took place in the SCM in the central and northern North Sea during the summer. Those workers also reported a distinct SCM in the northern North Sea where the depth was larger than ~40 m, i.e. areas where tidally induced mixing cannot break the stratified water column. The northern North Sea is relatively productive during the summer season with PP levels of ~0.5 - 0.9 g C m^{-2} d^{-1} (Weston et al, 2005; Fernand et al., 2013). However, few studies have been made of PP at the northern shelf-edge and the distribution of NP is unknown.

Biogeosciences Discuss., https://doi.org/10.5194/bg-2018-385
Manuscript under review for journal Biogeosciences
Discussion started: 7 September 2018

Here, we analyse the physical and biological processes affecting PP and NP during the stratified summer period across the shelf-edge in the north eastern North Sea based on data collected during the VERMIX cruise in July 2016. First, we describe the distribution of water masses, nutrients and vertical mixing in the area. Then, we present results from PP-incubations and, based on averaged representative photosynthetic parameters, calculate PP for the whole study area. Nitrate fluxes and NP are calculated and compared with PP to derive f-ratios. Finally, the implications for NP in the North Sea are discussed.

2 Methods

2.1 Study area and hydrographic measurements

The VERMIX study covered an area around the shelf-edge in the north eastern North Sea from the shallow shelf area (depth <50 m) across the western part of the Norwegian trench (~500 m) towards the coast of Norway (Fig. 1). In this study, we define the shelf-edge zone as being where depths are between 50 m and 100 m and refer to areas south and north of this zone as the shallow shelf area (<50 m) and the area off the shelf edge zone (>100m), towards Norway, respectively.

The cruise was carried out with R/V Dana (Technical University of Denmark) during the period 12 - 31 July 2016. Stations were placed along five transects between 56.2 - 57.8° N and along 8.25° E (Tr1), 7.75° E (Tr2), 7.25° E (Tr3), 6.75° E (Tr4) and 6.25° E (Tr5), respectively (i.e. ~25 km between transects). Wind and light conditions were typical for the period with windy conditions during the first week (along Tr1 and Tr2 with wind speeds up to 20 m s^{-1}) and relatively calm conditions during the rest of the cruise (Tr2-5). In total, 132 stations were sampled along the transects with a general distance between stations of 10 km. Additional stations along Tr2 and Tr4 decreased this distance to ~1 km. Measurements along these two transects were made several times during the cruise to examine temporal variability. Hydrographic measurements of conductivity, temperature and depth (CTD) were made with a Seabird SBE911 plus system, including two sets of temperature, conductivity and oxygen sensors (SBE43) and equipped with a SCUFA fluorometer, a PAR-sensor (Licor) and 12 Niskin bottles (30 l) for water sampling. All salinity values are reported as practical salinity (S_P) and referred to as salinity (S) and TEOS10 (IOC et al., 2010) was applied for calculating properties of seawater.

2.2 Measurements of turbulence and micro-structure

Micro-scale turbulence was measured with a loose-tethered free-fall Rockland Scientific International (RSI) VMP-250 microstructure vertical profiler equipped with two shear probes, a FP07 thermistor and a micro-conductivity sensor. Microstructure of temperature and salinity only supported the analysis of shear-induced turbulence and are not discussed further here. The profiler was also equipped with a CT- and pressure-sensor (JFE Advantech). The JFE-CTD data were binned in 0.1 dbar and the conductivity sensor was aligned with temperature by a delay of 0.14 s. Microstructure measurements were made at 512 Hz and stored at 64 Hz and the CT-sensor operated at 16 Hz. Turbulence profiles were obtained while the ship was freely drifting. In total, 253 casts down to about 5 m from the bottom, or to a maximum depth of 200 m above deeper areas, were made during the cruise. Every cast provided two shear-measurements and, in general, there was relatively small deviation between the two shear probes. Therefore, all measurements were included in the analyses and values from the two shear-probes were averaged. The dissipation rate (ε) of turbulent kinetic energy (TKE) was calculated with software provided by Rockland Scientific. Dissipation of TKE was estimated from below 10 m depth in order to exclude possible disturbances from the ship (depth of ship was 5.7 m) and analysed in bins of 8 seconds with 50% overlap following the method described by Wolk et al. (2002) and revised by Lueck (2016). The vertical turbulent diffusion coefficient (k_v) was estimated from the dissipation rate of TKE (Osborn, 1980):

$$k_v = \eta \frac{\varepsilon}{N^2} \tag{1}$$

with a mixing efficiency (η) equal to 0.2 and the Brunt-Väisälä frequency (N^2) determined by linear regression of density (ρ) with depth in 10 m intervals:

$$N^2 = -\frac{g}{\rho_0}\frac{\partial \rho}{\partial z} \tag{2}$$

where ρ_0 is a reference density (1027 kg m^{-3}) and g is the gravitational acceleration.

2.3 Measurements of nutrients and chlorophyll a

Water samples were taken at CTD stations from standard depths (5, 10, 30, 40, 60, 100, 200 m and close to the bottom). In addition, the depth of the subsurface chlorophyll a maximum (SCM) was sampled. At some stations, a distinct second chlorophyll peak or "extreme" (i.e, a subsurface chlorophyll a extremum, SCE) was observed above the SCM. In some cases, water for photosynthesis incubations and inorganic nutrient (nitrate, nitrite, ammonia, phosphorous and silicate) determination was taken from these SCEs. However, in this study we refer to the subsurface samples as from the SCM. Nutrient analysis was carried out by Aarhus University, Department of Bioscience. Chlorophyll a (GF/F filtered and extracted in 90% ethanol) was determined fluorometrically (Trilogy, Turner Designs) and used to calibrate the rosette mounted fluorometer (chlorophyll a is simply referred to as chlorophyll below). Detection limits for nitrite, nitrate, ammonia, phosphorous and silica were 0.04, 0.1, 0.3, 0.06 and 0.2 µM, respectively.

The background fluorescence measured in the deep profiles (>200 m) was considered to be generated by other material than chlorophyll a. Therefore, the fluorescence was averaged between 100-500 m at a deep station on Tr1 (57.83 °N, average value of 0.023 volt) and this value subtracted from the fluorescence signal (F) from surface waters at all of the stations. The chlorophyll concentration (chl, mg chl m^{-3}) was then determined from a linear regression between fluorescence (F) and filtered chlorophyll samples as chl = 3.23 F - 0.08 ($R^2 = 0.71$, n = 205).

2.4 Calculations of photosynthetic parameters and PP

Primary production (PP) was determined from incubations made with Photosynthetic Available Radiation (PAR) at 12 different light intensities from 0 - ~800 µE m^{-2} s^{-1}. In total, 64 incubations were made with water sampled from the surface and/or SCM at 41 stations. Total PP was then calculated according to Platt et al. (1980):

$$PP(chl, PAR) = P^B_{max}\, chl \left(1 - exp\left(-PAR\, \frac{\alpha^B}{P^B_{max}}\right)\right) exp\left(-PAR\, \frac{\beta^B}{P^B_{max}}\right) \qquad (3)$$

where the photosynthetic parameters (P^B_{max}, α^B and β^B) were determined by fitting the photosynthesis (P) vs. E curves generated from the incubations to Eq. (3) by a non-linear Levenberg-Marquardt least-squares routine (Press et al., 1992) and normalized with *in situ* chlorophyll a concentration obtained from the calibrated CTD-fluorescence measurement. The case without photo-inhibition, i.e. $\beta = 0$ (Webb et al., 1974), in general, resulted in a poorer representation of the data (except for six incubations where the photo-inhibition term was set to zero) and the incubation experiments were, therefore, analysed with the photo-inhibition term included in Eq. (3). These model fits were found to be in very good accordance with the incubations. The maximum rate of photosynthesis (defined as $P^B_{max}{}^*$) was calculated for each P vs. E curve.

Irradiation was measured continuously during the cruise and the hourly averaged insolation curve was scaled to equal the daily averaged photosynthetically available radiation (PAR) measured from the MODIS-Aqua satellite measurements (Frouin et al., 2014) where the daily averaged PAR for July 2016 in the study area (13-28 July, 6.2° - 8.3° E, 56.2° - 58° N) was 506 µ E m^{-2} s^{-1}. The vertical light extinction coefficient (k_d) was determined by linear regression of the log-transformed PAR-measurements from each CTD-cast. The average value from all the CTD-casts was found to be $k_d = 0.139 \pm 0.031$ m^{-1} (std.dev, n=177), corresponding to a 0.1 % PAR depth level of 50 m. The 0.1 % PAR depth level was in this study assumed to represent the bottom of the euphotic zone.

Average values of photosynthetic parameters in the surface layer (5 m) and in the SCM were calculated for the whole cruise and these average values were applied in the calculation of PP. Surface values were assumed to represent the photosynthetic parameters in the upper 10 m whereas average values from the SCM were assumed to represent the parameters for the water column below 10 m.

2.5 Vertical nutrient fluxes and f-ratios

Nitrate was depleted in the surface layer at almost every station and, therefore, nitrate was considered as the limiting nutrient. This assumption was also supported by the distribution of other nutrients. The nutricline was defined as the depth where nitrate equalled 0.5 µmol kg^{-1} (the threshold value had, in general, only a minor influence on the nutricline depth because of the nutrient depleted surface layer). In general, water samples were taken close to the nutricline, i.e. within +/- 10 m. However, to minimize the uncertainty of the nutricline depth estimate associated with the linear interpolation between two neighbouring water samples, the nutricline depth was found by linear interpolation between the corresponding potential density anomalies (σ_θ) of the sample depths, and the nutricline depth was then identified from the corresponding σ_θ in the CTD-profile (an example is shown in Fig. 6). This method is based on the assumption that the nitrate concentrations between two water samples are more closely related to water mass characteristics than linearly to depth changes, i.e. a sharp pycnocline, not resolved by the water samples, is taken into account when the nutricline depth is estimated by this method. A comparison was made from the whole data set between nutricline depth estimates based on linear interpolation using depth and potential density anomaly levels, respectively, and the difference between the two methods averaged -1.4 ± 2.5 m (std. dev., n=77) and the differences ranged between -9.9 - 2.4 m. Thus, in general, the depth level-based method resulted in a deeper nutricline (-1.4 m) than the applied σ_θ-method.

At all stations where nitrate was present, the nutricline was found to be located above the depth of the 0.1% PAR light level and, therefore, the flux of nitrate (F_{NO3}) for NP was found by calculating the maximum flux into the euphotic zone (only transports from vertical turbulent mixing were measured, thus, contributions from vertical advection were not considered). The vertical nitrate flux (F_{NO3}) due to turbulent mixing is defined as:

$$F_{NO3} = -k_v \frac{\partial NO_3}{\partial z} = -k_v \frac{\partial NO_3}{\partial \rho} \frac{\partial \rho}{\partial z} \tag{4}$$

where the vertical nitrate gradient is reformulated in terms of density (Sharples et al., 2007). By applying this reformulated relationship, together with the definition of the vertical turbulent diffusion coefficient in Eq. (1), an expression for the nitrate flux in terms of the measured dissipation rate of TKE becomes:

$$F_{NO3} = \frac{\eta\, \varepsilon\, \rho_0}{g} \frac{\partial NO_3}{\partial \rho} \tag{5}$$

The advantage of this expression, compared to simply applying k_v and the vertical nitrate gradient directly, is the dependence on the measured dissipation rate rather than the derived k_v-value. The latter includes the calculation of the Brunt Väisälä frequency (Eq. (2)). This term becomes close to zero in very turbulent conditions and, thereby, k_v becomes sensitive to rounding errors and other uncertainties in the measurements. The gradient of nitrate at a given depth was determined linearly from the nearest water sample depths.

PP was related to the vertical nitrate flux by estimating the f-ratio, calculated as: $f = \eta_{N:C} F_{NO3}/PP$, where $\eta_{N:C}$ is the Redfield ratio between nitrogen and carbon, i.e. 16:106.

3 Results

3.1 Water mass distributions

The northern North Sea is a region in which North Atlantic water transported towards the Skagerrak, water masses formed in the shallower part of the North Sea and outflowing low-saline water from the Baltic Sea come together. Water masses and the general circulation in the area have been described by Danielssen et al. (1990) based on measurements in the Skagerrak and the north eastern North Sea in 1990-91, and the general water mass characteristics they identified are included in the description below. The inflow of Atlantic water to the northern North Sea, in general, takes place between the Orkneys and Shetland, above the shelf east of the Shetland and in the deep Norwegian channel and the deep inflow in the Norwegian channel dominates during the summer period (Winther and Johannesen, 2006).

Atlantic water masses (AW) are characterized by salinities > 35 and can be further delineated as upper Atlantic water (AWu, S = 35.00 - 35.15 and T = 8 - 10 °C) and a slightly colder and more saline deeper Atlantic water mass (AWd, S = 35.15 - 35.32, T = ~7 - 10 °C, Fig. 1). The AWd was observed on the westernmost transects (Tr4 and Tr5) between 100 - 300 m along the shelf edge. High saline AWd was also present in the depth range 120 - 200 m on Tr1 (not shown). AWu was observed at the shelf edge at depths below 60 m on Tr2 - 5 whereas it was found at depths below 80 m on Tr1 (Fig. 2). An upward doming of the AWu was seen to reach to ~ 30 m between the shelf-edge and the Norwegian coast from where isotherms and isohalines tended to deepen towards Norway. Central North Sea water (CNSW, S = 34.80 - 35.0 and T = 8 - 10 °C), a mixture of Atlantic water and Scottish coastal water, was located above AWu and a distinct frontal zone between the two water masses was seen along the shelf-edge where bottom depths ranged between 40 and 60 m.

The influence of southern North Sea water (SNSW, S = 34.50 - 34.8, T = 8 - 12 °C and low nitrate concentrations (note the larger temperature interval in mid-summer than defined in Danielssen et al. (1990)), originating from the English Channel, was seen at the shallower stations (< 40 m) on all transects except Tr1, where warm subsurface water between 20 - 40 m indicated an influence from the Jutland coastal water mass (JCW, S = 32 - 34 and T = 10 - 15 °C). The surface mixed layer varied between 5 - 15 m with the lowest salinities seen in the Norwegian coastal water mass (S < 28) and the highest surface salinities being found above the well mixed shallow parts of the North Sea (S ~ 34.5).

A distinct subsurface oxygen maximum (O_2 > 240 µmol kg^{-1}) between ~15 - 35 m depth characterized the deeper area north of the shelf-edge whereas a less well-defined maximum was present above the shelf-edge and in the shallow North Sea (Fig. 2c). The bottom water (~20 - 60 m) in the shallow areas had a relatively low oxygen concentration, i.e., < 200 µmol kg^{-1}.

3.2 Chlorophyll a and nutrient distributions

The subsurface chlorophyll concentrations were relatively high (> 2 mg chl a m^{-3}) in the shallow northern North Sea (Fig. 3). A narrow well-defined subsurface chlorophyll maximum extended from the shelf-edge towards the Norwegian coast. The depth of the subsurface chlorophyll maximum tracked the nutricline from the shelf-edge, where the nutricline was separating the nutrient-depleted surface layer from the nutrient rich Atlantic water (Fig. 4a, b).

In general, a sharp nutricline separated the nutrient depleted surface layer from the nutrient rich Atlantic water with nitrate concentrations above 6 µmol kg^{-1}. For example, an increase from values below the detection limit (0.1 µmol nitrate kg^{-1}) to values above 2 µmol kg^{-1} was observed across a 5 m distance (35 - 40 m depth) at the shelf-edge on Tr4 (57.31 °N, not shown). The nutricline between CNSW and AWu was located at density-anomalies of ~27.3 kg m^{-3}, whereas the nutricline was located below the 26.5 kg m^{-3} isopycnal in areas influenced by SSW and Norwegian coastal water masses. Thus, high nutrient concentrations were found in the cold (< 8 °C) Atlantic water masses and low concentrations were associated with CNSW, SNSW and SSW.

3.2.1 Nitrate limitation and denitrification

Nitrate was not detectable at the southernmost stations south of 56.88° N at Tr5, 57.00° N at Tr4 and Tr3 and 57.21° N at Tr2, whereas the southernmost station at Tr1 showed detectable nitrate (0.2 - 0.3 µmol kg^{-1} between the surface and 30 m) at the near-coastal station, likely influenced by nutrient-rich JCW (Fig. 1). Bottom samples were typically made down to ~5 m from the bottom, i.e. within the benthic boundary layer, and, considering the relatively large turbulent diffusion coefficients in the benthic boundary layer, this supported that no detectable nitrate was present in the water column at the southernmost stations along Tr2-Tr5.

The assumption that nitrate was the limiting nutrient for phytoplankton was supported by the phosphate distributions, in that the N:P-ratio was found to be significantly below Redfield (16:1) at all stations and all depths, with the exception of a few samples above the shallow area (Fig. 4c). Nitrate depletion was observed at stations above the shallow southern North Sea, where excess phosphate compared to the Redfield N:P ratio suggested significant denitrification to be occurring. There was, in general, no indication of silicate limitation because relatively large values (up to 10 µmol kg^{-1}) were observed above the nitrate-depleted shallow area and low silicate values in the deeper part were also associated with low nitrate concentrations (not shown).

3.3 Mixing and vertical nitrate fluxes

Dissipation of TKE was low, i.e., < 10^{-9} W kg^{-1}, below ~40 m in the deeper areas north of the shelf-edge but increased by an order of magnitude above the shelf-edge, where values up to ~10^{-6} W kg^{-1} in the benthic boundary layer were recorded (Fig. 5a, b). Dissipation rates of TKE in the 20 – 40 m depth range varied between 10^{-8} - 10^{-9} W kg^{-1} above the deeper areas and increased to 10^{-7} - 10^{-8} W kg^{-1} above the shallow areas along Tr2. In the upper part of the water column, between 10 - 20 m depth, the dissipation rate of TKE increased to 10^{-5} - 10^{-7} W kg^{-1} due to mixing induced by wind and waves. The distribution of the vertical turbulent diffusion coefficient showed a characteristic pattern along all transects where very low k_v-values of <10^{-6} m^2 s^{-1} between 15 - 30 m depth characterized the deeper open areas, i.e. around the pycnocline, while elevated mixing was seen at the shelf-edge and in the ~10 m thick benthic boundary layer further south above the shallow shelf (Fig. 5c,d; note that the shallow turbulence profiles on Tr4 did not resolve the benthic boundary layer). The highest k_v-values above 10^{-4} m^2 s^{-1} were observed at the shelf edge and in the benthic boundary layer above the shallow part of the shelf.

Vertical nitrate fluxes were calculated for all stations where both nutrients and turbulence profiles were measured. An example is shown from a station at Tr5 (57.41° N, 86 m) north of the shelf edge zone (Fig. 6). The maximum vertical nitrate flux into the euphotic zone (50 m) was relatively small and the largest values (~0.2 mmol N m^{-2} d^{-1}) were associated with an increased mixing around 45 m (Fig. 6b), i.e. well below the nutricline depth at 35 m (this vertically localized increase in mixing around ~45 m was associated with the upper interface of a ~10 m thick and relatively homogeneous layer with a slightly lower temperature (not shown)). In general, the maximum vertical nitrate flux into the euphotic zone in the deeper parts along the five transects was located 5-10 m below the nutricline (Fig. 3, orange squares). However, the SCM was, in general, located at the nutricline (Figs. 3, 6a). Although the nitrate flux at this depth was relatively low, this showed the close relationship between SCM and nutricline depth. Elevated mixing at this station was observed towards the bottom (below the euphotic zone) in the benthic boundary layer and resulted in nitrate fluxes of ~3 mmol N m^{-2} d^{-1}.

3.4 Photosynthetic parameters

Photosynthetic parameters can vary as a function of sampling time and in situ light conditions. Therefore, in order to be able to compare the potential PP at different stations, we averaged photosynthetic parameters for the surface layer (5 m) and from the SCM, respectively. In total, 64 incubations were made. Fifty eight of the incubations were fitted with the photo-inhibition term whereas 6 incubations did not show any significant decrease for increasing light levels. Therefore, the inhibition term was excluded in these calculations. To make the data set representative for the whole study area, incubations from the closely spaced (1-3 km) stations on Tr2 were excluded (i.e. 14 stations between the two stations shown with incubations at Tr2 in Fig. 1) and, to reduce the impact from outliers, representative values are calculated as median and median absolute deviation values (Table 1).

The median chlorophyll concentrations at the surface and SCM were 0.16 and 1.68 mg chl a m^{-3}, respectively. This reflected the general increase in chlorophyll with depth observed over the entire area. The chlorophyll-normalized photosynthetic parameters of the photosynthetic rate constant (P^B_{max}) and the slope of the PE-curve (α^B) in the surface layer were 5.48 µg C (µg Chl h)$^{-1}$ and 0.041 µg C (µg Chl h µE m^{-2} s^{-1})$^{-1}$, respectively, and the corresponding values of P^B_{max} and α^B at the SCM were 2.33 and 0.027. Thus, P^B_{max} was significantly lower at the SCM, in general accordance with previous studies (see review in Richardson et al., 2016) whereas α^B showed a weak decrease with depth (with overlapping uncertainty intervals between the two depth levels). In general, α^B has been found to increase with depth (resulting in a more efficient photosynthetic response at low light levels) and inspection of the vertical distribution showed at tendency to higher values between 15 -25 m depth (i.e. 2 - 3 e-folding depth of PAR) and lower values below 30 m resulting in a lower median value from SCM level. It was noted that a similar pattern of α^B, with a subsurface maximum, has been observed at the European shelf in the Celtic Sea (Hickman et al., 2012).

There was a significant averaged photo-inhibition (β^B) at both depth levels (1.70 and 3.00 (10^{-3} μg C (μE m^{-2} s^{-1} $h)^{-1}$)). However, the average values at these depths were not significantly different. The maximum PP was characterized by $P^B{}_{max}{}^*$-values of 4.76 and 1.72 at the surface and SCM, respectively, corresponding to maximum PP at PAR-levels of 413 and 192 μE m^{-2} s^{-1}. The averaged parameters for the two depth levels of $P^B{}_{max}$, α^B and β^B were applied for calculating PP in the water column according to Eq. (3). A comparison was made between the resulting PE-curves and the maximum averaged PP from all the incubations (i.e. the $P^B{}_{max}{}^*$ and E_{max} in Table 1) and these values were found to fit the averaged curves for the two depth levels within 5% and, therefore, the PE-curve based on the values in Table 1 were assumed to be representative for the average conditions and applied in the calculations of PP for all the stations.

3.5 Vertically integrated chlorophyll a, PP and NP

The vertically integrated chlorophyll showed a local maximum south of the shelf-edge along all transects and a decrease in chlorophyll further south at the two westernmost transects, i.e. Tr4 and Tr5 (Fig. 7a). Relatively low values were observed in the area north of the shelf-edge with the exception of an area close to Norway where high values were observed. The averaged vertically integrated chlorophyll from all stations was 29.9 ± 7.8 mg chl a m^{-2} (std. dev., n = 128).

The distribution of vertically integrated total PP showed a similar pattern with increased PP-levels south of the shelf edge and a somewhat reduced PP further south at the two westernmost transects (Fig. 7b). A tendency to minimum values was observed at the shelf edge with an increasing tendency towards Norway with high PP-values being observed at a few stations near the Norwegian coast. The averaged vertically integrated PP from all stations was 476 ± 110 mg C m^{-2} d^{-1} (n=128).

The f-ratio was calculated for each station where nitrate and turbulence measurements were made and where nitrate was present in detectable concentrations. Elevated f-ratios were found along the shelf-edge on Tr2-Tr5 (nitrate fluxes were not measured at the shelf edge and at shallow stations at Tr1) and also near the Norwegian coast at Tr1 and Tr4 and low f-ratios characterized the open area between the shelf edge and Norway (Fig. 7c).

3.6 Distributions across the shelf-edge

A comparison of distributions of PP related parameters across the shelf-edge showed common trends over all five transects (Fig. 8). Vertically integrated chlorophyll and PP were relatively low, with values of ~20 mg chl a m^{-2} and 400 mg C m^{-2} d^{-1}, respectively, on the southernmost parts of the transects. A gradual northward increase towards maximum values (of ~60 mg chl a m^{-2} and >1000 mg C m^{-2} d^{-1}) was observed within a distance of ~20 km south of the shelf edge on Tr3 - Tr5. Transect 2 did not reach as far south of the shelf-edge. This could explain the southern maximum in chlorophyll and PP at Tr2. Transect 1 was influenced by nutrient rich JCW and this may be the reason for the high chlorophyll concentration (43 mg chl a m^{-2}) and PP (1746 mg C m^{-2} d^{-1}) at the southernmost station on this transect.

Relatively low values of ~20 mg chl a m^{-2} and 400 mg C m^{-2} d^{-1}, respectively, characterized the shelf-edge zone. These values increased slightly towards Norway to ~30 mg chl a m^{-2} and 5-600 mg C m^{-2} d^{-1}, respectively. High values were observed in Norwegian coastal water masses on Tr1 and Tr4, probably due to PP being stimulated by coastal upwelling. Stations on Tr2 and Tr4 were visited twice within one week. Significant temporal variation of chlorophyll and PP was observed (Fig 8a,b; bullets vs. open circles) between samplings. Chlorophyll increased by up to 40% above the shallow area near the shelf edge and a similar increase was seen in PP. Relatively large temporal variations were also seen in these parameters in the coastal Norwegian water masses.

A nutricline could, in general, not be identified above the shallow areas south of the shelf-edge except at two stations on Tr3 and Tr4 (cf. Fig. 2c, d, at both stations high nitrate concentrations of 0.9 - 1 µmol kg^{-1} were only measured at 5 m while low values of 0.1 - 0.3 µmol kg^{-1} were found below 10 m). The deepest nutricline depths (~40 m) were found near the shelf-edge. Nutricline depth decreased to ~20 m going northwards but then increased again in the coastal Norwegian water masses (Fig 8c).

Nitrate fluxes were generally very low (< 0.1 mmol N m^{-2} d^{-1}) in the deeper area north of the shelf edge due to low vertical mixing in the upper 50 m. However, elevated nutrient fluxes of ~1 mmol N m^{-2} d^{-1} were seen in the shelf edge zone and near the Norwegian coast. This resulted in f-ratios above 0.10 in these regions compared to < 0.02 for the remainder of the study area (Fig. 8d, e).

4 Discussion

The shelf edge was identified in this study as a potential area of localized NP during the stratified summer period in the north eastern North Sea. Very low f-ratios were estimated for most of the open water extending northwards from the shelf edge towards Norway. Likewise, little or no NP was estimated to be occurring in the nitrate depleted shallow reaches of the southern North Sea. Shelf edge areas have been shown to be regions of increased fishing activity (Sharples et al., 2013). We hypothesize that the abundance of fish in this area could be related to localized increased NP. It can also be noted that the north eastern shelf edge area is characterized by elevated fish species diversity (ICES, 2008), suggesting that the introduction of new nutrients to the euphotic region of the water column identified for this region may be influencing both food webs and ecosystem structure.

.

Localized NP at the shelf edge will also influence the oxygen concentration in subsurface water masses (Fig. 2). This can have a direct influence on ambient water with relatively low oxygen above the shallow shelf and influence conditions further downstream, where water masses from the shelf edge eventually reach the North Sea/Baltic Sea transition zone and contribute to bottom water ventilation in more eutrophic areas (Bendtsen et al., 2009).

Localized NP also implies that physical processes on relatively small spatial scales (~1 km) are important for modelling NP in the area. This is in general accordance with model studies where the resolution of physical processes at high spatial scales was found to be necessary to explain observed patterns of PP in the North Sea (Skogen and Moll, 2000). Holt et al. (2012) applied a high-resolution model of the whole North Sea area and showed that nutrient transports towards the shelf area were of primary importance for understanding PP and also for assessing the impact from climate change. Localized NP at the shelf edge in the north eastern North Sea may be representative for the open ocean - shallow shelf exchange of nutrients more generally. If so, then this NP may also impact nutrient conditions above the shallow central North Sea and may explain some of the recent decadal decline of PP in this area (Capuzzo et al., 2018).

4.1 Regenerated production above the shallow shelf

There was no measurable nitrate in the water column at stations south of the shelf-edge., i.e. an area where the whole water column was within the euphotic zone, i.e. < 50 m (Fig. 1). This indicates that nitrate sinks, i.e. biological consumption or denitrification, exceed nitrate sources, i.e. nitrification, nitrogen-fixation or advective supply during summer months in this region. Significant nitrification may take place in the water column (Clark et al. 2008; Zehr and Kudela, 2011) or in the sediment and, as pointed out in the work of Dugdale and Goering (1967), nitrate can, in this case, not be considered as a non-regenerated nutrient form in the euphotic zone. Yool et al. (2007) estimated a global specific nitrification rate of 0.2 d^{-1}, thus, even small concentrations of ammonium could lead to significant nitrification rates.

Concentrations of ammonium were, however, very low in the nitrate depleted area. For example, ammonium was undetectable at all nitrate-depleted stations on Tr5 and this indicated a relatively small contribution from nitrification in the euphotic zone. However, observed nitrification rates span a large range (Yool et al., 2007) and the importance of nitrification varies between ocean regions (Clark et al, 2008; Fawcett et al., 2015). Therefore, it remains an open question whether or not significant nitrification takes place in the euphotic zone in the area.

Diazotrophy constitutes another potential source of nitrogen to the nitrate-depleted surface layer and N_2-fixation has been measured in the southern North Sea at Dogger Bank (Fan et al., 2015). However, the estimated nitrogen fluxes from N_2-

fixation were very small compared to the relatively high PP. Increased nutrient fluxes and NP at the shelf-edge could also support PP in the ambient shallow areas through isopycnal transport of dissolved organic material. A substantial fraction of dissolved organic material remineralizes on time-scales of days to weeks (Bendtsen et al., 2015; Hansen and Bendtsen, 2014) and isopycnal transport of organic matter could then supply organic nitrogen from the shelf edge zone. Both the nitrification and isopycnal supply of organic material, thereby, potentially provide new nitrogen to the shallow area and this confuses the concept of nitrate-based new versus regenerated production here. However, nitrification in the euphotic zone would be based on regenerated production and, therefore, we consider PP to be regenerated production in areas without detectable nitrate in the water column.

Recycling of organic matter above the shallow shelf could, thereby, be maintained by regenerated organic matter in the water column or sediment and we analysed whether this was in accordance with estimated carbon and nitrogen pools. The high biomass in the shallow area, indicated by chlorophyll concentrations of ~2 - 4 mg chl a m^{-3} in the bottom layer, would rapidly consume a regenerated pool of inorganic nitrogen. The regenerated cycling could, in principle, originate from the winter concentration of nitrate of ~6 mmol DIN m^{-3} in the area (Pätch and Kühn, 2008) and, when accounting for the large denitrification in the shallow area ranging within 0 - 4 mmol DIN m^{-3} (Fig. 4c), this would correspond to a pool of more than 2 mmol DIN m^{-3} available for establishing the phytoplankton biomass. Assuming a Redfield C:N molar ratio of 6.6 and a C:chlorophyll a ratio of 1 mg C/50 mg chl a, this would equal ~3 mg chl a m^{-3}, in general accordance with the observed levels of <1 and ~4 mg chl a m^{-3} in the surface and bottom layers, respectively. Relatively low oxygen concentrations in the bottom layer also suggested an active bacterial respiration (Fig. 2c) to be occurring here. Thus, regenerated production could be maintained and explained by recycling of an initial nutrient pool from early spring.

4.2 Photosynthetic parameters and PP

Estimates of PP based on photosynthetic parameters from ^{14}C-incubations and in situ conditions of light and chlorophyll rely on several critical assumptions, including photosynthetic parameters, the distribution of chlorophyll, light conditions and nutrient-carbon relationships. Photosynthetic parameters from individual incubation experiments were well described by the PP-model (Eq. (3)) so uncertainty is mainly related to the spatial and temporal variability of these parameters. Photosynthetic parameters are bulk parameters describing the physiological response of the phytoplankton community as a whole to a given a photon flux. Thus, both algae composition and actual fitness of the cells contribute to the observed range of these parameters.

The values reported here (Table 1) are comparable with those found in previous studies in the North Sea (e.g. Weston et al., 2005). However, variability of the photosynthetic parameters is critical for the PP calculations. The uncertainty of the surface value of $P^B_{max}{}^*$ of ~±30% implies a corresponding uncertainty in PP. This spatial variability is not accounted for in this study where all stations were assumed to be represented by a common set of photosynthetic parameters. Thus, using a common set of photosynthetic parameters is a simplification even within this relatively small study area, and similar limitations would probably apply to other PP estimates for the North Sea area. These considerations illustrate why a better understanding of the distributions of photosynthetic parameters and the factors underlying these distributions is a prerequisite for improved estimates of PP on regional and larger scales.

Additional uncertainties are related to the chlorophyll distribution due to the application of an overall relationship (i.e. linear regression) between CTD-fluorescence and measurements of GF/F filtered chlorophyll samples. Similarly, the light extinction coefficient was assumed to be constant and, although a relatively small variation was found in the area, this together with the assumption of constant daily PAR-distribution during the days in July, also can introduce errors in the local PP-estimates. Finally, estimates of new production imply a conversion from nitrate to carbon and a fixed ratio may not be representative for the different communities in the area.

The general limitations above could have been accounted for by increasing the number of incubations at each station but that would have been at the expense of the spatial coverage of the data set. Thus, the PP and NP estimates are limited by the above simplifications and should, therefore, be interpreted as a general representation of PP in the area, reflecting the combined influence from the vertical chlorophyll distribution and PAR.

4.3 Nutrient fluxes and NP at the shelf edge zone

The largest vertical nitrate fluxes of 0.5 - 1.5 mmol N m^{-2} d^{-1} were localized above the shelf edge where increased mixing in the bottom layer intersected the nutricline within the euphotic zone. Similar large nitrate fluxes have been observed along the European shelf where tidal-induced (Sharples et al., 2001; located in the English Channel) or wind-induced mixing (Williams et al., 2013; Celtic Sea) lead to vertical fluxes of 1 - 2 mmol N m^{-2} d^{-1}. Significantly larger fluxes have also been observed above steep bathymetric gradients (Tweddle et al., 2013). Wind and tidal mixing may also provide energy for intensified mixing along the north eastern shelf edge in the North Sea, although the present study did not resolve the specific cause for increased mixing. Shelf-edge zones are dynamic areas where cross-shelf exchange may occur due to many different dynamic processes (Huthnance, 1995).

Mixing from tides (Sharples et al, 2007; 2009) and breaking internal waves (e.g. Burchard and Rippeth, 2008) has been shown to be important for vertical nutrient fluxes in shelf areas. These potential sources of mixing were analysed here from two time series stations (data not shown) at the shelf edge taken around spring tide and neap tide (20-21 and 29-30 July, according to OTIS tidal predictions; Egbert and Erofeeva, 2002). Elevated mixing of nutrients into the euphotic zone due to tides or short term mixing events was not observed at these locations.

Other processes may be important on the north eastern shelf edge due to the large in- and outflow of Atlantic water masses. It is interesting to note that the deepening of the nutricline from the open areas towards the shelf edge follows the slope of the pycnocline. The slope of the pycnocline implies, via the thermal wind equations, an increased eastward baroclinic velocity component with depth, in accordance with the general cyclonic circulation in the area. Thus, deepening of the nutricline can potentially be explained as a dynamic response to a shelf-edge current transporting Atlantic water into the area.

The conditions across the shelf edge observed during the stratified summer season may, therefore, be considered as a stable quasi-stationary system where mixing at the shelf edge, associated with a deep nutricline and nutrient rich bottom currents, provide nutrients to the euphotic zone stimulating localised new production in this area. Isopycnal mixing may provide organic matter for increased regenerated production above the nitrate-depleted shallow shelf area and also, together with upwelling along the Norwegian coast, provide fresh organic material to the euphotic zone off the shelf edge towards Norway.

4.4 Nutrient fluxes north of the shelf edge

The position of the SCM was closely related to the depth of the nutricline (e.g. Fig. 3 and 6) and located in the middle of the euphotic zone (average nutricline depth from all stations was 29.1 ± 9.7 m, n = 83). The maximum nitrate flux was found at depth levels between 3.4 m above and 23.1 m below the nutricline but, on average, it was located 6.4 ± 7.7 m (n=73) below the nutricline depth (e.g., Fig. 6). Thus, the maximum nitrate flux was, in general, within the euphotic zone but significantly below the SCM (Fig. 3). This implies that internal recycling from below the SCM towards the surface of regenerated nitrogen is necessary for maintaining the phytoplankton biomass in the upper layer. Considering the relatively low vertical mixing rates around the SCM (e.g., a turbulent diffusion coefficient of $<5\cdot10^{-5}$ m^2 s^{-1} implies a time scale of ~3 weeks for mixing across a 10 m thick layer, Fig. 5), this indicates that other transport processes within the euphotic zone are important in this area, e.g. diel vertical migration of plankton (e.g., Raven and Richardson, 1984).

Nutrient fluxes and NP increased close to the Norwegian coast (Fig. 8). This was in accordance with chlorophyll a estimates (Hu et al., 2012) based on daily images from the MODIS-Aqua satellite: A large algal bloom was observed 6 July and covered the area off the southern-most part of Norway. An image from 20 July showed increased chlorophyll levels near the Norwegian coast. Although our observations were made more than 12 nautical miles from the coast, the elevated chlorophyll and PP values at Tr1 and Tr4 are likely related to these features. A tendency to a thicker chlorophyll layer around the SCM and a deeper nutricline at Tr4 and Tr5 also indicate increased mixing, upwelling, or eddy activity near the coast. Mixing processes along the Norwegian shelf edge may, therefore, similarly contribute to NP in the area.

5 Conclusion

Relatively high PP and chlorophyll concentrations of 476 mg C m^{-2} d^{-1} and 30 mg chlorophyll m^{-2}, respectively, characterized the stratified north eastern North Sea in July 2016. The greatest values were found above the shallow shelf and near the Norwegian coast. Turbulence measurements showed maximum dissipation rates of TKE in the benthic boundary layer above the shallow shelf area and elevated mixing above the shelf edge zone, whereas very low vertical mixing rates characterized the deeper open area. Chlorophyll was concentrated in a subsurface chlorophyll maximum located near the nutricline and, on average, about 6 m above the depth of the maximum vertical nitrate flux in the deeper area north of the shelf edge. Chlorophyll was concentrated in the bottom layer above the shallow and nitrate depleted shelf area. Significant NP was found above the shelf-edge where vertical nitrate fluxes of 0.5 - 1.5 mmol N m^{-2} d^{-1} implied f-ratios above 0.10 whereas very low nutrient fluxes characterized the open area above the Norwegian Trench (f-ratios < 0.02). This localized NP along the shelf edge, potentially represents an important key to understanding temporal variability of biological production, ecosystem structure and diversity in this productive area.

Author contribution

Measurements of primary production and turbulence were carried out by KR and JB, respectively, and both analyzed the data and prepared the manuscript.

Acknowledgements

We thank captain and crew on-board R/V Dana for very helpful assistance and support during the cruise and Eik Ehlert Britch for technical support. This study was supported by funding for ship-time by the Danish Centre for Marine Research. The Carlsberg foundation provided support for the turbulence instrument (CF15-0301). The Villum foundation provided support for the cruise and analysis of the measurements. Analyses were supported by Danish National Science Foundation via its support of the Center for Macroecology, Evolution, and Climate (grant no. DNRF96). Satellite derived PAR-data was obtained from NASA Goddard Space Flight Center, Ocean Ecology Laboratory, Ocean Biology Processing Group (2014): MODIS-Aqua Ocean Color Data, http://doi.org/10.5067/AQUA/MODIS/L3M/PAR/2018 and http://doi.org/10.5067/AQUA/MODIS/L3M/CHL/2018, (Accessed on 2018/05/10).

References

Bendtsen, J., Gustafsson, K. E., Söderkvist, J., and Hansen, J. L. S.: Ventilation of bottom water in the North Sea – Baltic Sea transition zone, J. Mar. Sys., 75, 138–149, doi: 10.1016/j.jmarsys.2008.08.006, 2009.

Bendtsen, J., Hilligsøe, K. M., Hansen, J. L. S., and Richardson K.: Analysis of remineralisation, lability, temperature sensitivity and structural composition of organic matter from the upper ocean, Prog. Oceanogr., 130, 125–145, doi: 10.1016/j.pocean.2014.10.00, 2015.

Burchard, H. and Rippith, T.: Generation of bulk shear spikes in shallow stratified tidal seas, J. Phys. Oceanogr., 39, 969–985, 2009.

Capuzzo, E., Lynam, C. P., Barry, J., Stephens, D., Forster, R. M., Greenwood, N., McQuatters-Gollop, A., Silva, T., van Leeuwen, S. M., Engelhard, G. H.: A decline in primary production in the North Sea over 25 years, associated with reductions in zooplankton abundance and fish stock recruitment, Glob. Change Biol., 24, e352–e364, doi: 10.1111/gcb.1391, 2018.

Clark, D. R., Rees, A. P., and Joint, I.: Ammonium regeneration and nitrification rates in the oligotrophic Atlantic Ocean: Implications for new production estimates, Limnol. Oceanogr., 53, 52–62, 2008.

Danielssen, D. S., Edler, L., Fonselius, S., Hernroth, L., Ostrowski, M., Svendsen, E., and Talpsepp, L.: Oceanographic variability in the Skagerrak and Northern Kattegat, May–June, 1990. ICES J. Mar. Sci., 54, 753–773, 1997.

Dugdale, R. C., and Goering, J. J.: Uptake of new and regenerated forms of nitrogen in primary productivity. Limnol. Oceanogr., 12, 196–206, 1967.

Egbert, Gary D., and Erofeeva, S. Y.: Efficient inverse modeling of barotropic ocean tides, J. Atm. Ocean. Tech., 19, 183–204, 2002.

Eppley, R. W., and Peterson, B. J.: Particulate organic matter flux and planktonic new production in the deep ocean, Nature, 282, 677–680, 1979.

Fan, H., Bolhuis, H., and Stal, J.: Drivers of the dynamics of diazotrophs and denitrifiers in North Sea bottom waters and sediments, Front. Microbiol., 6, 738, doi: 10.3389/fmicb.2015.00738, 2015.

Fawcett, S. E., Ward, B. B., Lomas, M. W., and Sigman, D. M.: Vertical decoupling of nitrate assimilation and nitrification in the Sargasso Sea, Deep-Sea Res. I, 103, 64–72, 2015.

Fernand, L., Weston, K., Morris, T., Greenwood, N., Brown, J. and Jickells, T.: The contribution of the deep chlorophyll maximum to primary production in a seasonally stratified shelf sea, the North Sea, Biogeochemistry, 113, 153–166, doi: 10.1007/s10533-013-9831-7, 2013.

Frouin, R., McPherson, J., Ueyoshi, K., and Franz, B. A.: A time series of photosynthetically available radiation at the ocean surface from SeaWiFS and MODIS data, Remote Sensing of the Marine Environment II. doi: 10.1117/12.981264, 2012.

Hansen, J. L. S., and Bendtsen, J.: Seasonal bottom water respiration in the North Sea–Baltic Sea transition zone: rates, temperature sensitivity and sources of organic material, Mar. Ecol.-Prog. Ser., 499, 19–34, 2014.

Hickman, A. E., Moore, C. M., Sharples, J., Lucas, M. I., Tilstone, G. H., Krivtsov, V., Holligan, P. M.: Primary production and nitrate uptake within the seasonal thermocline of a stratified shelf sea, Mar. Ecol.-Prog. Ser., 463, 39–57, 2012.

Holt, J., and Proctor, R.: The seasonal circulation and volume transport on the northwest European continental shelf: A fine-resolution model study, J. Geophys. Res., 113, C06021, doi: 10.1029/2006JC004034, 2008.

Holt, J., Wakelin, S., Lowe, J., and Tinker, J.: The potential impacts of climate change on the hydrography of the northwest European continental shelf, Prog. Oceanogr., 86, 361–379, 2010.

Holt, J., Butenschön, M., Wakelin, S. L., Artioli, Y., and Allen, J. I.: Oceanic controls on the primary production of the northwest European continental shelf: model experiments under recent past conditions and a potential future scenario, Biogeosciences, 9, 97–117, doi: 10.5194/bg-9-97-2012, 2012.

Hu, C., Lee, Z., and Franz, B. A.: Chlorophyll-a algorithms for oligotrophic oceans: A novel approach based on three-band reflectance difference, J. Geophys. Res. 117, C01011, doi: 10.1029/2011JC007395, 2012.

Huthnance, J. M.: Circulation, exchange and water masses at the ocean margin: the role of physical processes at the shelf edge, Prog. Oceanogr. 35, 353–431, 1995.

ICES: Report of the ICES Advisory Committee 2008. Book 6: North Sea. International Council for the Exploration of the Sea (ICES), 2008.

IOC, SCOR and IAPSO: The international thermodynamic equation of seawater – 2010: Calculation and use of thermodynamic properties. Intergovernmental Oceanographic Commission, Manuals and Guides No. 56, UNESCO (English), 196pp, 2010.

Lueck, R.: Calculating the rate of dissipation of turbulent kinetic energy, RSI Technical Note 028, Rockland Scientific International, Victoria, Canada, 18 pp, 2016.

Osborn, T. R., Estimate of the local rate of vertical diffusion from dissipation measurements, J. Phys. Oceanogr., 10, 83–89, 1980.

Pätsch, J. and Kühn, W.: Nitrogen and carbon cycling in the North Sea and exchange with the North Atlantic – A model study. Part I. Nitrogen budget and fluxes, Cont. Shelf Res., 28, 767–787, 2008.

Pätsch, J., Burchard, H., Dieterich, C., Gräwe, U., Gröger, M., Mathis, M., Kapitza, H., Bersch, M., Moll, A., Pohlmann, T., Su, J., Ho-Hagemann, Ha T. M., Schulz, A. Elizalde, A., and Eden, C.: An evaluation of the North Sea circulation in global and regional models relevant for ecosystem simulations, Ocean Model., 116, 70–95, 2017.

Platt, T., Gallegos, C. L., and Harrison, W. G.: Photoinhibation of photosynthesis in natural assemblages of marine phytoplankton, J. Mar. Res. 38, 687–701, 1980.

Press, W.H., Teukolsky, S.A., Vetterling, W.T., Flannery, B.P.: Numerical Recipes in FORTRAN: The Art of Scientific Computing, Press Syndicate of the University of Cambridge, USA, 1986.

Raven, J. A. and Richardson, K.: Dinophyte flagella: a cost-benefit analysis, New Phytol., 98, 259–276, 1984.

Richardson, K., Visser, A.W., and Pedersen, F. B.: Subsurface phytoplankton blooms fuel pelagic production in the North Sea, J. Plankton Res., 22, 1663–1671, 2000.

Richardson, K., Bendtsen, J., Kragh, T., and Mousing, E. A.: Constraining the distribution of photosynthetic parameters in the global ocean, Front. Mar. Sci., 3, 269, doi: 10.3389/fmars.2016.00269, 2016.

Røed, L. P., and Fossum, I.: Mean and eddy motion in the Skagerrak/northern North Sea: insight from a numerical model, Ocean Dynam., 54, 197–220, doi:10.1007/s10236-003-0076-1, 2004.

Scott, B. E., Sharples, J., Ross, O. N., Wang, J., Pierce, G. J. and Camphuysen, C. J.: Sub-surface hotspots in shallow seas: fine-scale limited locations of top predator foraging habitat indicated by tidal mixing and sub-surface chlorophyll, Mar. Ecol.-Prog. Ser., 408, 207–226, doi: 10.3354/meps08552, 2010.

Sharples, J., Moore, C. M., Rippeth, T. P., Holligan, P. M., Hydes, D. J., Fisher, N. R., and Simpson, J. H.: Phytoplankton distribution and survival in the thermocline, Limnol. Oceanogr., 46, 486–496, 2001.

Sharples, J., Tweddle, J. F., Green, J. A. M., Palmer, M. R.,Kim, Y.-N., Hickman, A. E., Holligan, P. M., Moore, C. M., Rippeth, T. P., Simpson, J. H., and Krivtsov, V.: Spring-Neap Modulation of Internal Tide Mixing and Vertical Nitrate Fluxes at a Shelf Edge in Summer, Limnol. Oceanogr., 52, 1735–1747, 2007.

Sharples, J., Moore, C. M., Hickman, A. E., Holligan, P. M., Tweddle, J. F., Palmer, M. R., and Simpson, J. H.: Internal tidal mixing as a control on continental margin ecosystems, Geophys. Res. Lett., 36, L23603, doi:10.1029/2009GL040683, 2009.

Sharples, J., Ellis, J. R., Nolan, G., and Scott, B. E.: Fishing and the oceanography of a stratified shelf sea, Progr. Oceanogr., 117, 130–139, 2013.

Skogen, M. D., and Moll, A.: Interannual variability of the North Sea primary production: comparison from two model studies, Cont. Shelf Res., 20, 129–151, 2000.

Tweddle, J. F., Sharples, J., Palmer, M. R., Davidson, K., and McNeill, S.: Enhanced nutrient fluxes at the shelf sea seasonal thermocline caused by stratified flow over a bank, Progr. Oceanogr., 117, 37–47, 2013.

Volk, T., and Hoffert, M.I.: Ocean carbon pumps: Analysis of relative strengths and efficiencies in ocean-driven atmospheric CO_2, In: The Carbon Cycle and Atmospheric CO_2: Natural Variations Archean to Present, Geophysical Monograph Series, vol. 32. Sundquist, E.T., Broecker, W.S. (Ed.), AGU, Washington, DC, pp. 99 –110, 1985.

Webb, W. L., Newton, M., and Starr, D.: Carbon dioxide exchange of Alnus rubra. A mathematical model, Oecologia, 17, 281–291, 1974.

Weston, K., Fernand, L., Mills, D. K., Delahunty, R. and Brown, J.: Primary production in the deep chlorophyll maximum of the central North Sea, J. Plankt. Res., 27, 909–922, 2005.

Williams, C., Sharples, J., Mahaffey, C., and Rippeth, T.: Wind-driven nutrient pulses to the subsurface chlorophyll maximum in seasonally stratified shelf seas, Geophys. Res. Lett., 40, 5467–5472, doi:10.1002/2013GL058171, 2013.

Winther, N. G., and Johannessen, J. A.: North Sea circulation: Atlantic inflow and its destination, J. Geophys. Res., 111, C12018, doi:10.1029/2005JC003310, 2006.

Wolk, F., Yamazaki, H., Seuront, L., and Lueck, R. G.: A new free-fall profiler for measuring bio-physical microstructure, J. Atmos. Ocean. Tech., 19, 780–793, 2002.

Yool, A., Martin, A. P., Fernández, C., and Clark, D. R.: The significance of nitrification for oceanic new production. Nature, 447, 999–1002, 2007.

Zehr, J. P., and Kudela, R. M.: Nitrogen cycle of the open ocean: From genes to ecosystems, Ann. Rev. Mar. Sci., 3, 197–225, 2011.

Figure 1 VERMIX station map of the five transects in the north eastern North Sea. CTD stations (bullets) and stations where ^{14}C-incubations for primary production were used for estimating photosynthetic parameters in the area (white circles). Horizontal gray bars (Tr2-5) show the separation between nitrate-deplete and nitrate-replete areas. Water masses in the area are indicated (see text).

Figure 2 Distributions along Tr4 of (a) potential temperature (°C, colours and white contours, additional contours above 16 °C in 0.5 °C intervals), (b) salinity (psu, colours and white contours, additional contours between 26-34 in 0.5 psu intervals) and contours of potential density anomalies (kg m^{-3}, orange lines) and, (c) oxygen (µmol kg^{-1}, colours and black contours). Vertical lines show location of the CTD-measurements.

Figure 3 Distributions of chlorophyll a (mg chl m^{-3}, colours and black contours, additional white contours are shown in intervals of 2 mg chl m^{-3}) along Tr1-Tr5 (a-e). Nutricline depths (red bullets) and depths with maximum nitrate flux into the euphotic zone (orange squares) were calculated at each station where water samples (black triangles) and turbulence profiles were made, respectively. Note the different latitude-intervals in the figures.

Figure 4 (a) Potential temperature-salinity diagram of all CTD-measurements and (b) a high-saline subset of the measurements (small grey bullets). Water sample concentrations of nitrate are shown with large bullets in (a,b) (µmol kg^{-1}, colour bar). Contour lines show isopycnals of potential density anomalies and selected water masses are indicated. (c) Nitrate vs phosphate for all water samples. The total water depth is shown with colours (m) and the relationship $[NO_3^-] = \eta_{N:P} [PO_4^-]$, $\eta_{N:P} = 16:1$, is shown with a grey dashed line.

Figure 5 Turbulence measurements along Tr2 (a,c) and Tr4 (b,d). (a,b) Logarithm (Log_{10}) of dissipation of turbulent kinetic energy (W kg^{-1}) and (b,d) calculated vertical turbulent diffusion coefficient (m^2 s^{-1}).

Figure 6 Vertical profiles from a station at the shelf edge of (a) potential density anomaly, chlorophyll a and nitrate (bullets; sample depths, line; interpolated values by the σ_θ-method) and (b) dissipation of TKE, turbulent diffusion coefficient and the vertical turbulent nitrate flux. The nutricline depth (DNO3) and depth of the euphotic zone (0.1% PAR) are shown.

Figure 7 (a) Vertically integrated chlorophyll a (mg chl a m^{-2}) and (b) primary production (mg C m^{-2} d^{-1}). Values are proportional to the diameter of the circles. (c) Distribution of f-ratios in the euphotic zone (colours, no unit).

Figure 8 Distributions along the five transects of (a) vertically integrated chlorophyll a (mg chl a m^{-2}), (b) primary production (mg C m^{-2} d^{-1}), (c) nutricline depth (m), (d) maximum nitrate flux into the euphotic zone (mmol N m^{-2} d^{-1}) and (e) f-ratio in euphotic zone. Repeated stations on Tr2 and Tr4, separated in time by about a week, are shown with bullets and open circles.

Figure 9 Sketch of conditions across the shelf edge zone during summer. The largest f-ratios are found above the shelf-edge zone where the nutricline (D_{NO3}) gets in contact with elevated mixing near the bottom. Deep waters are characterized by high nitrate concentration whereas surface water and water above the shallow North Sea (NS) are nitrate depleted.

Table 1. Distribution of photosynthetic parameters. Median values, and absolute median deviations (number of samples *n* in parenthesis) of photosynthetic parameters at 5 m below the surface and at the SCM.

Depth level	Depth	$\mathbf{P^B_{max}}^*$	$\mathbf{P^B_{max}}$	$\boldsymbol{\alpha^B}$	$\boldsymbol{\beta^B}$	$\mathbf{E_{max}}$	**Chl a**
	[m]	[µg C (µg Chl h)$^{-1}$]	[µg C (µg Chl h)$^{-1}$]	10^{-2}·[µg C·(µg Chl h µE m^{-2} s^{-1})$^{-1}$]	10^{-3}·[µg C (µE m^{-2} s^{-1} h)$^{-1}$]	[µE m^{-2} s^{-1} h]	[mg chl m^{-3}]
Surface	*5.0± 0.0 (23)*	*4.76 ± 1.33 (19)*	5.48 ± 0.87 (23)	4.10 ± 0.90 (23)	1.70 ± 1.70 (23)	413 ± 76 (19)	0.16 ± 0.06 (23)
SCE	*27.0± 5.0 (25)*	*1.72 ± 0.38 (24)*	2.33 ± 0.64 (25)	2.70 ± 0.80 (25)	3.00 ± 0.90 (25)	192 ± 26 (24)	1.67 ± 0.73 (25)

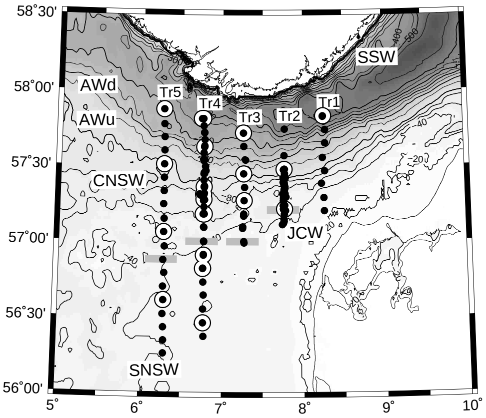
58°30'
58°00'
57°30'
57°00'
56°30'
56°00'
5°
6°
7°
8°
9°
10°
SSW
AWd
AWu
CNSW
SNSW
JCW
Tr5
Tr4
Tr3
Tr2
Tr1
400
500
40
20
80
40

Figure 1

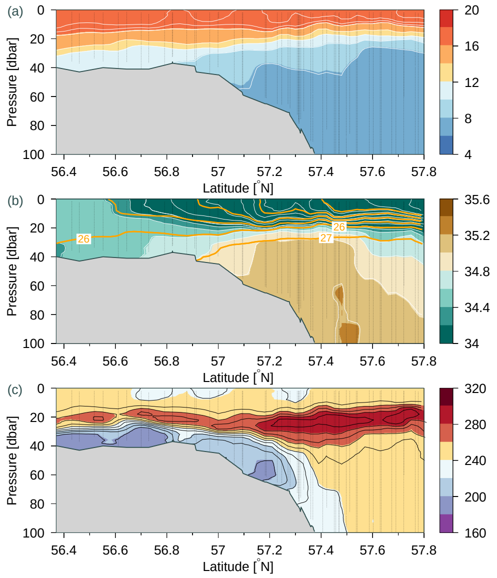
(a)
Pressure [dbar]
0
20
40
60
80
100
56.4
56.6
56.8
57
57.2
57.4
57.6
57.8
Latitude [°N]
20
16
12
8
4
(b)
Pressure [dbar]
26
26
27
Latitude [°N]
35.6
35.2
34.8
34.4
34
(c)
Pressure [dbar]
Latitude [°N]
320
280
240
200
160

Figure 2

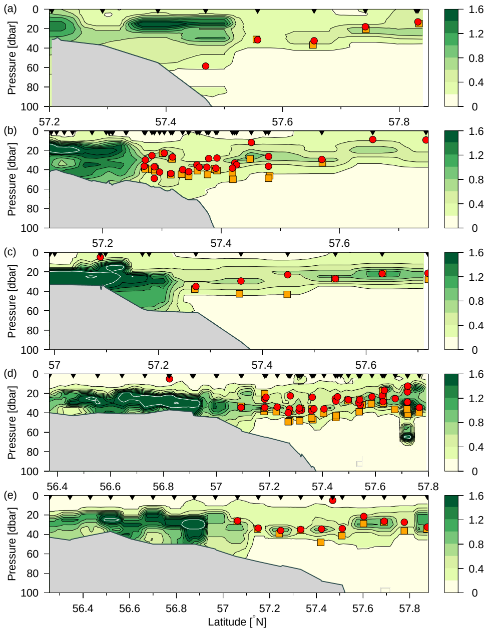
(a)
(b)
(c)
(d)
(e)
Pressure [dbar]
0
20
40
60
80
100
57.2
57.4
57.6
57.8
57
56.4
56.6
56.8
57.2
1.6
1.2
0.8
0.4
0
Latitude [°N]

Figure 3

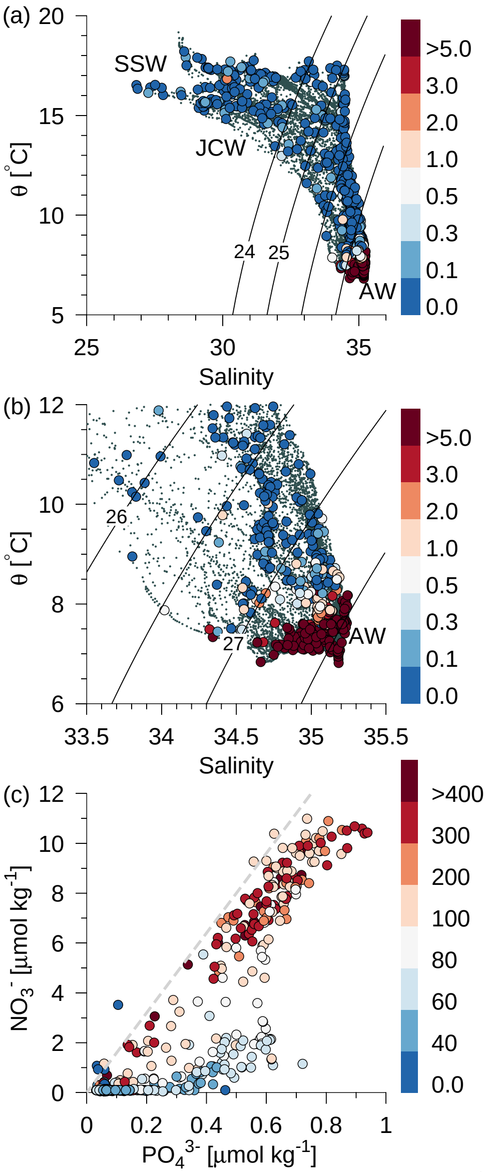
(a)
20
15
10
5
θ [°C]
SSW
JCW
AW
24
25
25
30
35
Salinity
>5.0
3.0
2.0
1.0
0.5
0.3
0.1
0.0
(b)
12
10
8
6
θ [°C]
26
27
AW
33.5
34
34.5
35
35.5
Salinity
>5.0
3.0
2.0
1.0
0.5
0.3
0.1
0.0
(c)
12
10
8
6
4
2
0
NO_3^- [μmol kg^{-1}]
0
0.2
0.4
0.6
0.8
1
PO_4^{3-} [μmol kg^{-1}]
>400
300
200
100
80
60
40
0.0

Figure 4

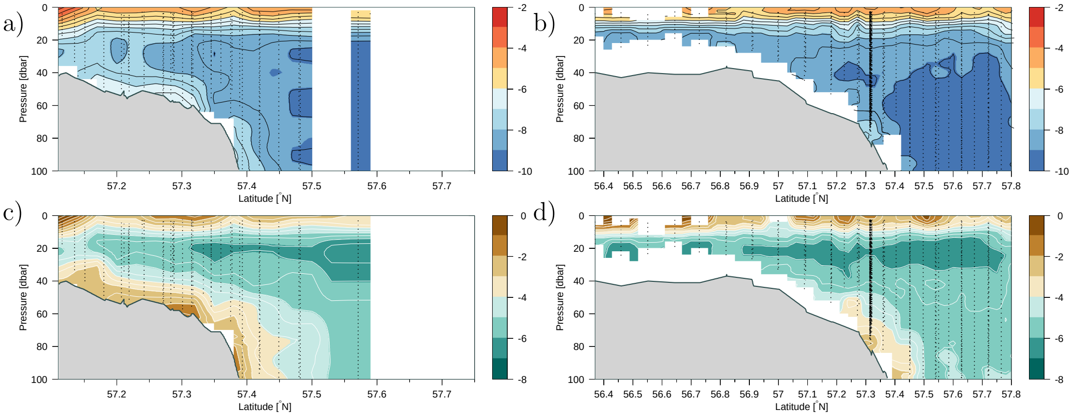
a)
b)
c)
d)
Pressure [dbar]
0
20
40
60
80
100
57.2
57.3
57.4
57.5
57.6
57.7
Latitude [˚N]
56.4
56.5
56.6
56.7
56.8
56.9
57
57.1
57.2
57.3
57.4
57.5
57.6
57.7
57.8
-2
-4
-6
-8
-10
0
-2
-4
-6
-8

Figure 5

Biogeosciences Discuss., https://doi.org/10.5194/bg-2018-385
Manuscript under review for journal Biogeosciences
Discussion started: 7 September 2018

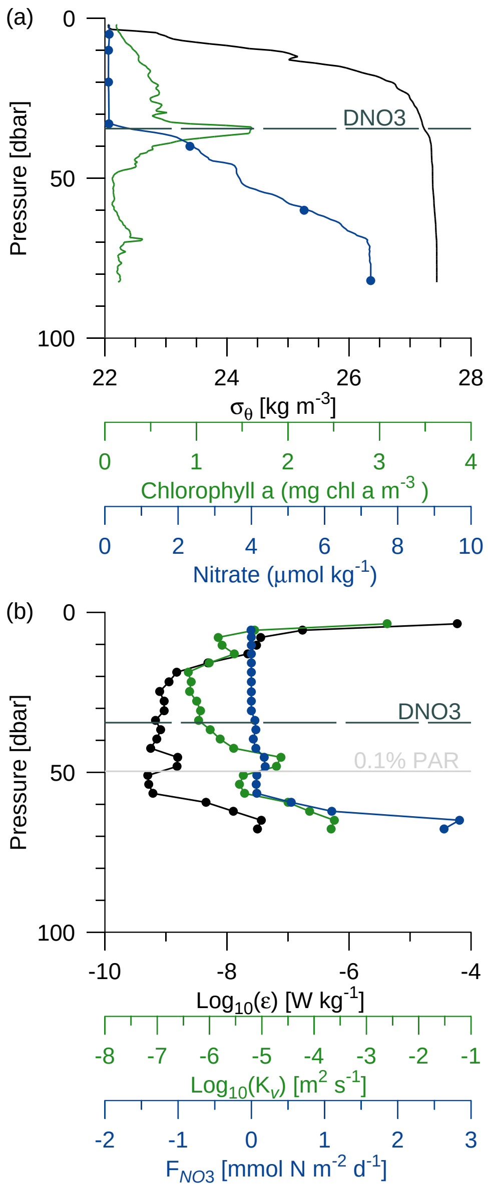

Figure 6

Biogeosciences Discuss., https://doi.org/10.5194/bg-2018-385
Manuscript under review for journal Biogeosciences
Discussion started: 7 September 2018

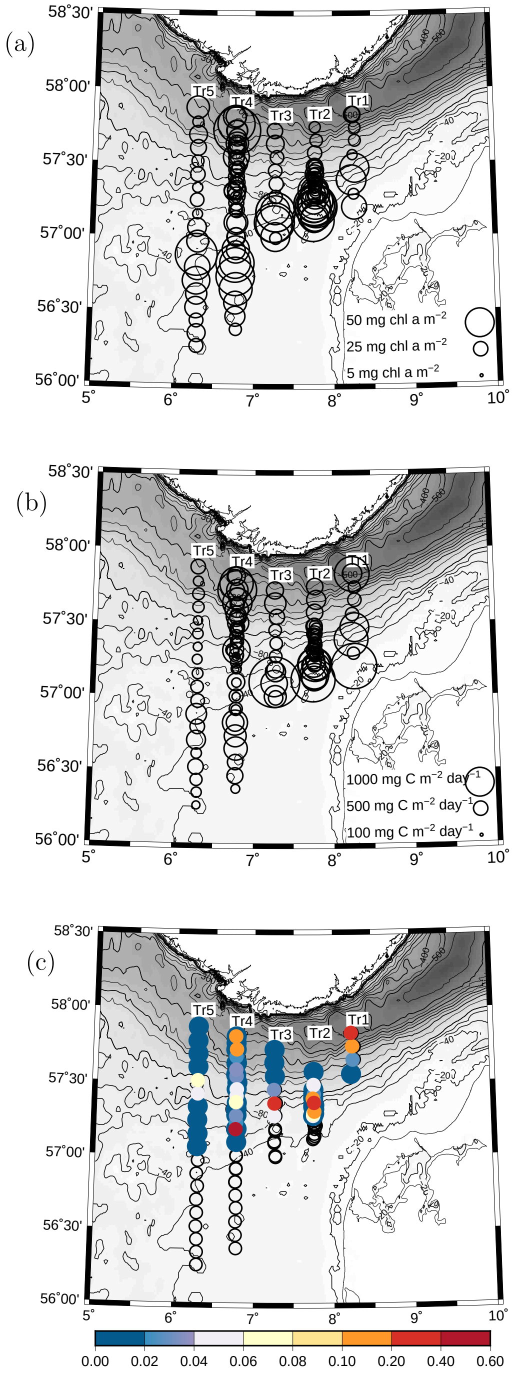

Figure 7

Biogeosciences Discuss., https://doi.org/10.5194/bg-2018-385
Manuscript under review for journal Biogeosciences
Discussion started: 7 September 2018

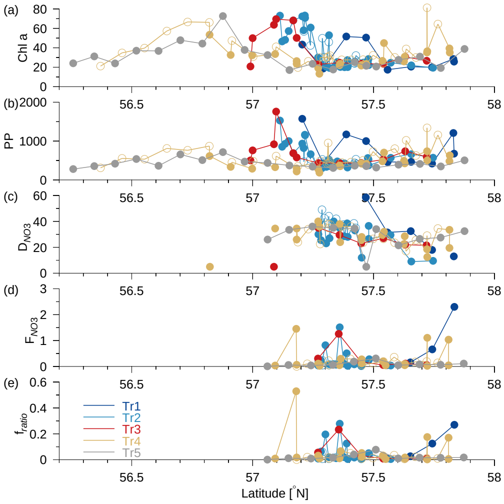

Figure 8

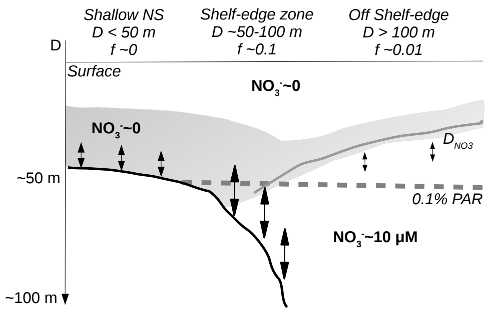
Shallow NS
D < 50 m
f ~0
Shelf-edge zone
D ~50-100 m
f ~0.1
Off Shelf-edge
D > 100 m
f ~0.01
D
Surface
NO_3^-~0
NO_3^-~0
D_{NO3}
~50 m
0.1% PAR
NO_3^-~10 µM
~100 m

Figure 9